Interaction Between Equally Charged Membrane Surfaces Mediated by Positively and Negatively Charged Macro-Ions

Šárka Perutková · Mojca Frank · Klemen Bohinc ·
Goran Bobojevič · Jasna Zelko · Blaž Rozman ·
Veronika Kralj-Iglič · Aleš Iglič

Abstract In biological systems, charged membrane surfaces are surrounded by charged molecules such as electrolyte ions and proteins. Our recent experiments in the systems of giant phospholipid vesicles indicated that some of the blood plasma proteins (macro-ions) may promote adhesion between equally charged membrane surfaces. In this work, theory was put forward to describe an IgG antibody-mediated attractive interaction between negatively charged membrane surfaces which was observed in experiments on giant phospholipid vesicles with cardiolipin-containing membranes. The attractive interactions between negatively charged membrane surfaces in the presence of negatively and positively charged spherical macro-ions are explained using functional density theory and Monte Carlo simulations. Both, the rigorous solution of the variational problem within the functional density theory and the Monte Carlo simulations show that spatial and orientational ordering of macro-ions may give rise to an attractive interaction between negatively charged membrane surfaces. It is also shown that the distinctive spatial distribution of the charge within the macro-ions (proteins) is essential in this process.

Keywords Macro-ion · Electric double layer · Functional density theory · Monte Carlo simulation · Adhesion

Š. Perutková · K. Bohinc · A. Iglič (✉)
Laboratory of Biophysics, Faculty of Electrical Engineering, University of Ljubljana, Tržaška 25, 1000 Ljubljana, Slovenia
e-mail: ales.iglic@fe.uni-lj.si

M. Frank · B. Rozman
Department of Rheumatology, University Medical Center Ljubljana, Vodnikova 62, 1000 Ljubljana, Slovenia

K. Bohinc
Faculty of Health Studies, University of Ljubljana, Poljanska 26a, 1000 Ljubljana, Slovenia

G. Bobojevič
Laboratory of Telecommunications, Faculty of Electrical Engineering, University of Ljubljana, Tržaška 25, 1000 Ljubljana, Slovenia

G. Bobojevič · J. Zelko · V. Kralj-Iglič
Laboratory of Clinical Biophysics, Faculty of Medicine, University of Ljubljana, 1000 Ljubljana, Slovenia

Introduction

Membrane micro- and nanovesiculation is a major yet underappreciated mechanism playing a vital role in the development of cells and organisms. Microvesicles and nanovesicles derived from cell membranes as the final products of the budding process (Greenwalt 2006) were found to have important roles in vascular hemostasis (Martinez et al. 2005; Müller et al. 2003; Sims et al. 1989), promotion of cancer (Whiteside 2005) and inflammation (Cerri et al. 2006; Distler et al. 2005). Increased levels of circulating microvesicles were found in patients suffering from cardiovascular disorders (Diamant et al. 2004), cancer (Janowska-Wieczorek et al. 2006) and autoimmune diseases (Berckmans et al. 2002; Combes et al. 1999; Dignat-George et al. 2004) and associated with an increased risk of thromboembolic events. Cellular membranes serve as a permeability barrier to charged particles (micro- and nanovesicles, lipoproteins or DNA). Electroporation-based methods may help in transmembrane transport of such charged particles (Kandušer et al. 2009). A typical example is transfection of cells with plasmid DNA. In some cases the transport of charged particles across the membrane may be coupled to

dynamic membrane deformation (Deserno 2004; Fleck and Netz 2004; Góźdź 2007) driven by electrostatic interactions between the membrane and the charged particles (Fošnarič et al. 2009; Lin et al. 2003). Specifically, attachment of small positively charged liposome to negatively charged membrane can result in strong local membrane bending and liposome encapsulation (Hägerstand et al. 1999) or plasma proteins which can mediate partial encapsulation of small charged liposome by equally charged membrane (Pavlič et al. 2009). In the case of membrane vesiculation, the mechanisms underlying the formation of microvesicles and their shedding from cellular membranes are poorly understood. Our recent experiments with giant phospholipid vesicles (GPVs) indicate that certain isolated plasma proteins such as β_2-glycoprotein I and IgG antibodies (Frank et al. 2009; Urbanija et al. 2007), human plasma itself (Frank et al. 2008) as well as low-molecular weight heparins (Frank et al. 2009) may cause the membrane buds to adhere back to the negatively charged parent membrane and thereby prevent them from becoming free vesicles. As the exposure of negatively charged phospholipids in the external leaflet of cellular membranes precedes the membrane microvesiculation process (Dachary-Prigent et al. 1995), it was hypothesized that by mediating an attractive interaction between negatively charged membranous structures blood plasma proteins or heparins may suppress the microvesiculation process and therefore act as anticoagulant and antitumor agents (Frank et al. 2009; Urbanija et al. 2008a).

The attractive interaction between equally charged surfaces could not be predicted within the mean-field electrostatic theory (Poisson–Boltzmann theory). Attraction between equally charged surfaces may be driven by particle–particle correlations (i.e., inter-ionic correlations) (Carnie and McLaughlin 1983; Kirkwood and Shumaker 1952; Kjellander 1996; Netz 2001; Oosawa 1968). Also, orientational ordering (intra-ionic correlation) of macroions (counter-ions) with internal charge distribution may lead to attractive forces between equally charged surfaces (Bohinc et al. 2004; Kim et al. 2008; May et al. 2008; Urbanija et al. 2008b).

In our previous study (Urbanija et al. 2008b) the functional density theory was used to describe attractive interactions between two negatively charged surfaces. However, this previous study was limited to the system of two equally charged membrane surfaces separated by the solution of counter-ions only. In order to theoretically describe the observed IgG antibody-mediated attractive interactions between negatively charged membranes, our present study is extended to a more general case of intermittent solution being composed of two kinds of macro-ions, i.e., positively and negatively charged macro-ions with internal spatially distributed electric charge. In such a way, our theoretical description of adhesion between two negatively charged membranes in the presence of polyclonal IgG antibodies becomes more realistic since the actual composition of the intermittent solution is taken into account.

To study the systems of charged particles interacting with charged surfaces, Monte Carlo (MC) simulations are widely used hand in hand with different theoretical approaches describing point-like counter-ions (Hatlo and Lue 2009; Moreira and Netz 2002), finite-sized counterions (Bhuiyan and Outhwaite 2009; Ibarra-Armenta et al. 2009; Tresset 2008) as well as the spatial distribution of charge within counter-ions and co-ions (Kim et al. 2008; May et al. 2008; Urbanija et al. 2008b).

In this study, MC simulations and the functional density theory were used to describe the system of two charged surfaces with intermediate solution of negatively and positively charged macro-ions, taking into account the spatial charge distribution within the single macro-ion (i.e., intra-ionic charge correlation) but not inter-ionic correlations. An example of experimentally observed attractive interactions between equally charged GPV surfaces mediated by positively and negatively charged macro-ions, such as mixtures of polyclonal serum IgG antibodies, is also given.

Experimental and theoretical results of the present study indicate that in the systems containing both positively and negatively charged macro-ions with internal charge distribution attractive interactions between equally charged membranes can occur. It is shown that the positional and orientational ordering of macro-ions with internal spatially distributed charges is crucial for this process.

Materials and Methods

Human IgG Antibodies

Polyclonal IgG antibodies from serum of a healthy donor as well as serum of a patient with syphilis, who gave written informed consent, were isolated by affinity purification on a 2-ml protein G column (ImmunoPure[G] IgG purification kit; Pierce Chemical, Rockford, IL), using the protocol recommended by the manufacturer, and equilibrated against phosphate-buffered saline (PBS, pH 7.4), in a desalting column. The concentration of IgG antibodies was determined using a protein assay (Bio-Rad Laboratories, Hercules, CA) with IgG antibody used as a protein standard. The final concentrations of IgG antibodies in the experiments ranged 0.21–0.40 mg/ml (for details, see "Experimental results").

The presence of anticardiolipin antibodies (aCL) in the sera was determined by anticardiolipin ELISA (Čučnik et al. 2004). The serum of the syphilitic patient contained high titers of aCL. No aCL were detected in the healthy donor serum.

Preparation of GPVs

GPVs were prepared in a 0.2 mol/l sucrose solution by the modified electroformation method (originally proposed by Angelova et al. 1992), as described in Ambrožič et al. (2006). For GPVs containing 10% weight ratio of cardiolipin (CL-GPVs), synthetic phospholipids 1,1′,2,2′-tetraoleoyl cardiolipin, 1-palmitoyl-2-oleoyl-sn-glycero-3-phospho-choline (POPC) and plant-derived cholesterol (Avanti Polar Lipids, Alabaster, AL), all dissolved in a 2:1 chloroform/methanol mixture at the concentration of 1 mg/ml, were combined in the proportion 1:7:2 (v/v/v). For GPVs containing 20% weight ratio of phosphatidylserine (PS-GPVs), synthetic 1-palmitoyl-2-oleoyl-sn-glycero-3-phosphoserine, POPC and plant cholesterol, all dissolved in chloroform at the concentration of 1 mg/ml, were combined in the proportion 1:3:1 (v/v/v). After electroformation, 3 ml of GPV/sucrose suspension was rinsed out of the electroformation chamber with 5 ml of 0.192 mol/l glucose solution mixed with 0.277 mol/l PBS (v/v = 9/1). GPVs were left overnight to sediment under gravity.

Observation of Adhesion Between GPVs

Experiments were performed at room temperature, pH 7.4. Polyclonal IgG antibodies (5 μl) were added to the solution of GPVs (45 μl) in a home-made observation chamber, described in Ambrožič et al. (2006). Adhesion between GPVs in the presence of IgG antibodies was observed by an inverted microscope (Zeiss Axiovert 200; Carl Zeiss MicroImaging, Jena, Germany) with phase-contrast optics and recorded with a VisiCam 1280 camera (Visitron Systems, Puchheim, Germany). For ionic strength experiments, GPV suspensions of different ionic strengths were prepared by combining different volumes of GPV/sugar/PBS suspension with different volumes of 0.1 mol/l NaCl solution. Under the phase-contrast microscope GPVs containing sucrose solution appeared darker in comparison to the surrounding sugar/PBS/NaCl solution because of the differences in refraction indices of the solutions.

Measurement of Adhesion Between GPVs

An average effective angle of contact, measured as described in Frank et al. (2008), was used to quantitatively compare the strength of GPV adhesion for different IgG antibody preparations or at different ionic strengths. Larger average effective angle of contact corresponds to stronger adhesion between GPVs, while smaller average effective angle of contact reflects weaker adhesion between GPVs.

The average effective angle of contact was determined as a mean value of many (on average 500) effective angles of contact between adhering GPVs measured in the phase-contrast microscope images, using Image J software (National Institutes of Health, Bethesda, MD; http://rsb.info.nih.gov/ij). These images were acquired in the time interval of 25–30 min after the addition of IgG antibodies using MatLab 7.1 (MathWorks, Natick, MA) or Meta-Morph Imaging System (Visitron Systems) software.

Statistical Analysis

Statistical analysis was performed using SPSS 15.0 software (SPSS, Inc., Chicago, IL). For an average effective angle of contact between adhering GPVs, descriptive statistical parameters (average, standard deviation and frequency distribution) were calculated. Student's t test was used to compare the average effective angle of contact between GPVs in the presence of different IgG antibodies.

Experimental Results

IgG Antibodies Induce Adhesion of Negatively Charged GPVs

Polyclonal IgG antibodies from syphilitic patient serum, which contained high titers of infectious-type aCL, induced the adhesion of CL- (Fig. 1) as well as PS-GPVs (Table 1). The strength of adhesion of CL- and PS-GPVs mediated by
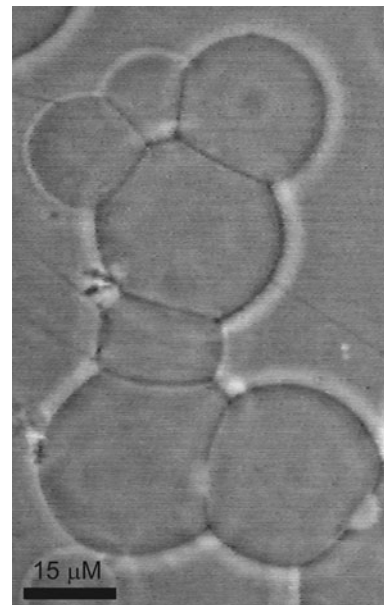

Fig. 1 Adhesion of negatively charged cardiolipin-containing membranes of giant phospholipid vesicles (GPVs) in the presence of IgG antibodies from a syphilitic patient with high titers of anticardiolipin antibodies. The adhesion started within 10 min after the addition of IgG antibodies to GPV suspension. The adhesion process between GPVs is very quick: Neighboring GPVs adhere within seconds after the adhesion process starts

Table 1 Influence of ionic strength on the average effective angle of contact between negatively charged CL- or PS-GPVs in the presence of IgG antibodies from syphilitic patient serum, containing high titers of aCL

Ionic strength (mmol/l)	Average effective angle of contact (°)	
	CL-GPVs	PS-GPVs
26	111 ± 18	
43		41 ± 10
50	68 ± 20	
86		No adhesion

Concentrations of IgG antibodies were 0.40 mg/ml in the CL-GPV experiment and 0.25 mg/ml in the PS-GPV experiment

syphilitic IgG antibodies was ionic strength-dependent. Specifically, as shown in Table 1, smaller average effective angles of contact between adhering GPVs were determined at higher ionic strengths, meaning that the strength of adhesion is decreased with increasing ionic strength of GPV-IgG antibody suspension.

In the presence of polyclonal IgG antibodies from a healthy donor ($c = 0.21$ mg/ml) containing no aCL, the average effective angle of contact between CL-GPVs was large ($81° \pm 21°$), indicating strong adhesion of CL-GPVs mediated by healthy donor IgG antibodies. Although large, this adhesion was significantly smaller compared to the adhesion of CL-GPVs in the presence of syphilitic IgG antibodies ($c = 0.21$ mg/ml, average effective angle of contact $87° \pm 21°$; $P < 0.0001$). No adhesion could be observed when PBS alone was added to the GPV suspension to control the effect of background solution (in which antibodies were dissolved) on GPV adhesion (Fig. 2).

In the experiments we used polyclonal IgG antibodies from a syphilitic patient with high titers of aCL as well as polyclonal IgG antibodies from healthy donor serum containing no aCL. Since aCL of infectious type from the
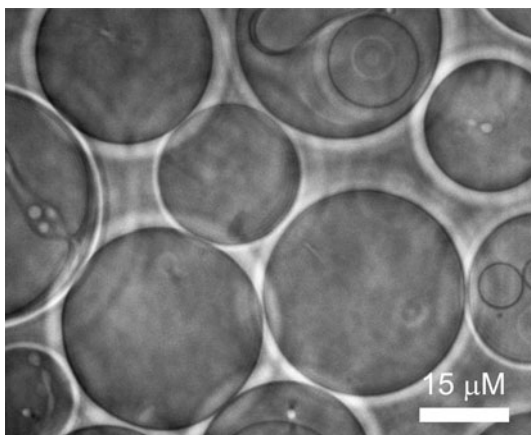

Fig. 2 Cardiolipin-containing giant phospholipid vesicles treated with PBS alone (as background control) do not adhere at all

syphilitic patient sera directly target CL membranes, they would effectively cross-link CL-GPVs through a specific antigen–antibody interaction, which is primarily electrostatic in nature (Celli et al. 1999). This would explain the significantly larger adhesion of CL-GPVs observed in the presence of syphilitic compared to healthy donor IgG antibodies. Anyway, experimental data suggest that aCL are not the only serum IgG antibodies involved in the adhesion process between negatively charged GPVs since (1) syphilitic IgG antibodies mediated the adhesion between PS-GPVs whose membrane was not composed of CL and (2) CL-GPVs adhered also in the presence of IgG antibodies from a healthy donor containing no aCL. It is also indicated that IgG antibody-mediated adhesion of negatively charged GPVs is mainly electrostatically driven since it decreases and is finally lost with increasing ionic strength of GPV-IgG antibody suspension.

Several experimental and theoretical approaches have been described in the literature to study possible orientations that IgG antibodies could attain during physical adsorption to a charged surface, taking into account the distribution of charge in the antibody molecule (Chen et al. 2003; Zhou et al. 2003). In these studies specific IgG antibodies with known amino acid sequence and structure were used, such as 1IGY and 1IGT (codes from Research Collaboratory for Structural Bioinformatics Protein Data Bank [RCSB PDB]). Meanwhile, we used human serum-derived IgG antibodies purified on Protein G affinity columns, which are a population of IgG antibodies with different antigenic specificities. It could be expected that a proportion of these antibodies would have negatively or positively charged termini of Fab fragments or would bear charged antigen-binding sites (paratopes). Due to a symmetric dimeric Y- or T-shaped molecular structure with two identical Fab termini/paratopes at the tips of Y (T), IgG antibodies with charged Fab termini would represent a poly-ion with a dimeric distribution of internal (positive/negative) charge. Such IgG antibodies would, according to the theoretical studies and MC simulations given here, induce a cross-bridging attractive interaction between neighboring negatively charged membranes (see also Urbanija et al. 2008b). To estimate the possible charge distributions within Fab termini of IgG antibodies, we explored the amino acid sequences and structural data of different IgG molecules or their Fab fragments available in the RCSB PDB (http://www.pdb.org/pdb/home/home.do). The content of charged amino acids was compared between Fab N′ terminal domain and whole IgG antibody/Fab fragment molecule. IgG antibody/Fab fragments with net positive (PDB codes, e.g., 1IGY and 3HZK) as well as net negative (PDB codes, e.g., 2G75 and 1SBS) Fab termini were found within the RCSB PDB.

The presented system with negatively charged membranes of GPVs immersed in the solution containing

purified serum IgG antibodies represents a feasible experimental model for studying mediated attractive interactions between planar charged surfaces due to the orientational and positional ordering of macro-ions in the electric field between two charged surfaces.

It can be concluded from this model that the experimental data indicate that serum IgG antibodies induce adhesion between negatively charged phospholipid membranes. We suggest that this adhesion is mainly electrostatically driven as it decreases and is finally lost by increasing the ionic strength of the solution between negatively charged membranes.

Theory

In this work, a functional density approach (Kralj-Iglič and Iglič 1996) was used to describe an aqueous solution containing positively and negatively charged spherical macro-ions with internal charge distribution. In the model the charge of a single macro-ion is composed of two negative or positive charges (each of valency Z), separated by the distance, l, equal to the diameter of the sphere. The solution of the macro-ions is sandwiched between two large, planar negatively charged surfaces (Fig. 3) with the surface charge density σ. The distance between the two charged surfaces is D. We assume that there is no electric field behind the charged surfaces, which is equivalent to the condition of electroneutrality of the whole system. The electrostatic field varies only in the normal direction between the two charged surfaces (i.e., in x direction). The spherical macro-ions are characterized by a positional and an orientational degree of freedom. The term $n_i(x)$ refers to the number density of macro-ion centers. If the center of the macro-ion is located at position x, then the two point charges of the macro-ion are located at geometrically opposite sides, i.e., at $x + s$ and $x - s$, with a certain probability density, $p_i(s|x)$, for each value of s. By taking into account that the two point charges of a single macro-ion are indistinguishable, all possible orientations of macro-ion can be described by the values of s in the interval $0 \leq s \leq l/2$ (see Fig. 3). Therefore, the probability density should satisfy the following conditions:

$$\frac{2}{l} \int\limits_0^{l/2} \mathrm{d}s \, p_i(s|x) = 1 \tag{1}$$

and

$$p_i(s|x) = 0 \tag{2}$$

for any x and $s > l/2$. Here, $i = +$ stands for positively charged macro-ions and $i = -$, for negatively charged macro-ions.
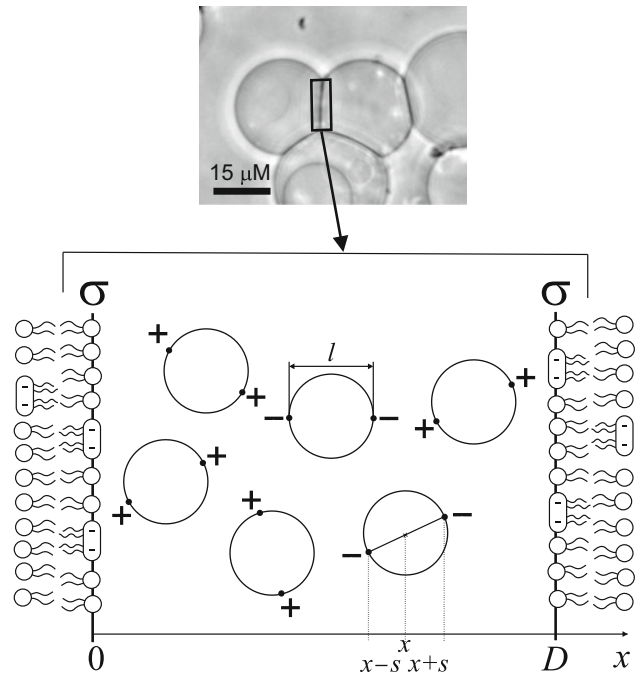

Fig. 3 Schematic presentation of two equally charged planar surfaces interacting in an electrolyte solution that contains spherical macro-ions. Phase-contrast image shows the adhering surfaces of two neighboring GPVs in the presence of syphilitic IgG antibodies, and it is used as an illustration. The separation between the individual charges of each spherical macro-ion is denoted by l and the distance between two surfaces, D. The position of each charge within the macro-ion is described by the reference position of the center of macro-ion (x) and the distance $s \leq l/2$

The free energy of the system, F, is composed of the energy stored in the electrostatic field, F_{elstat}, as well as the translational, F_{transl}, and orientational entropy of the spherical macro-ions, F_{orient} (Kralj-Iglič and Iglič 1996; May et al. 2008; Urbanija et al. 2008b):

$$F = F_{\mathrm{elstat}} + F_{\mathrm{transl}} + F_{\mathrm{orient}} \tag{3}$$

The first contribution to the free energy is the energy of the electrostatic field $\mathbf{E}(x)$:

$$\frac{F_{\mathrm{elstat}}}{AkT} = \frac{1}{2AkT}\varepsilon\varepsilon_0 \int\limits_0^D \mathbf{E}^2 \mathrm{d}V = \frac{1}{8\pi l_{\mathrm{B}}} \int\limits_0^D \Psi'(x)^2 \mathrm{d}x \tag{4}$$

where $\Psi(x) = e_0\varphi(x)/kT$ is the reduced electric potential, φ is the electric potential, e_0 is the elementary charge, ε is the dielectric constant of the water, ε_0 is the permittivity of the free space, k is the Boltzmann constant, T is the absolute temperature, A is a unit area of the charged surface and l_B is the Bjerrum length in water:

$$l_B = e_0^2/4\pi\varepsilon\varepsilon_0 kT \cong 0.7 \text{ nm} \tag{5}$$

Translational entropy of macro-ions (see, e.g., Bohinc et al. 2008) is derived from the number of all possible spatial

arrangements of the centers of macro-ions in the space between both charged membrane surfaces, W. Introducing W into the Boltzmann equation for the entropy $S_{transl} = k \ln W$ (Hill 1986; Dill and Bromberg 2003) and using the Stirling approximation yields $F_{transl} = -T S_{transl}$ in the form (Bohinc et al. 2008)

$$\frac{F_{transl}}{AkT} = \int_0^D \left[\sum_{i=\pm} n_i(x) \ln \frac{n_i(x)}{n_0} + 2n_0 - \sum_{i=\pm} n_i(x) \right] dx \quad (6)$$

where $n_i(x)$ is the number density of the centers of the macro-ions of type i and n_0 is the bulk number density of positively and negatively charged spherical macro-ions.

Orientational entropy (May et al. 2008; Urbanija et al. 2008b) is given by

$$\frac{F_{orient}}{AkT} = \int_0^D dx \sum_{i=\pm} n_i(x) \frac{2}{l} \int_0^{l/2} p_i(s|x)[\ln p_i(s|x) + U(x)] ds \quad (7)$$

where the integral of $[p_i(s|x) \ln p_i(s|x)]$ over all possible ds gives the orientational entropy of single macro-ion at position x. The orientational entropy of all macro-ions is then calculated by summation over all positive and negative macro-ions in the system. In continuous limit this is done by integration over $n_i(x) dx$. In Eq. 7 we introduced the external reduced potential of the charged wall

$$U(x) = \begin{cases} 0, & l/2 \le x \le D - l/2 \\ \infty, & \text{elsewhere} \end{cases} \quad (8)$$

which ensures that the spherical macro-ions could not penetrate through the membrane surfaces. In thermal equilibrium, the free energy $F = F[n_i(x), p_i(s|x)]$ (Eq. 3) adopts its minimum with respect to the functions $n_i(x)$ and $p_i(s|x)$. The condition for the minimum of the functional F is given by its variation:

$$\delta F(n_i(x), p_i(s|x)) = 0 \quad (9)$$

From the variational procedure (Bohinc et al. 2009; May et al. 2008), considering Eq. 1 and the constraint that the total number of the macro-ions of each kind in the whole system is constant, follow the expression for conditional probability:

$$p_i(s|x) = \frac{\exp(-iZ\Psi(x+s) - iZ\Psi(x-s))}{\langle \exp(-iZ\Psi(x+s) - iZ\Psi(x-s)) \rangle} \quad (10)$$

and the number densities of the centers of the positive and negative macro-ions

$$n_i(x) = n_0 \langle \exp(-iZ\Psi(x+s) - iZ\Psi(x-s)) \rangle \exp(-U(x)) \quad (11)$$

where $n_i(x)$ is defined in the region $l/2 \le x \le (D - l/2)$ (Bohinc et al. 2009; May et al. 2008) and the average value

of any given function $g(s)$ in the region $0 \le s \le l/2$ is defined as

$$\langle g(s) \rangle = \frac{2}{l} \int_0^{l/2} g(s) ds \quad (12)$$

The local charge densities at coordinate $x[\rho_i(x)]$ contain the contributions from the charges of the macro-ions having their centers located in the region $[x - l/2, x + l/2]$:

$$\frac{\rho_i(x)}{Ze_0} = \langle n_i(x-s, s) + n_i(x+s, s) \rangle \quad (13)$$

where $n_i(x-s, s) = n_i(x-s)p_i(s|x-s)$ is the contribution of the macro-ions with their centers located on the left side of x at the positions $(x-s)$, while $n_i(x+s, s) = n_i(x+s)p_i(s|x+s)$ is the contribution of the macro-ions with their centers located on the right side of x at the positions $(x+s)$. We defined $n_i(x, s) = n_i(x)p_i(s|x)$. By inserting Eqs. 10 and 11 into Eq. 13, we yield

$$\frac{\rho_i(x)}{Ze_0} = 2n_0 \langle \exp(-U(x+s) - iZ\Psi(x) - iZ\Psi(x+2s)) \rangle \quad (14)$$

and the total local charge density $\rho(x)$ is defined by the sum

$$\rho(x) = \sum_{i=+,-} i\rho_i(x) \quad (15)$$

By inserting $\rho(x)$ from Eq. 15 into the Poisson equation,

$$\Psi''(x) = -4\pi l_B \rho(x)/e_0 \quad (16)$$

we obtain the integro-differential equation for the reduced electric potential:

$$\psi''(x) = -8\pi l_B Z n_0 \\ \sum_{i=\pm} i \langle \exp(-U(x+s) - iZ\Psi(x) - iZ\Psi(x+2s)) \rangle \quad (17)$$

The boundary conditions are given at both charged surfaces:

$$\Psi'(x=0) = -\sigma \frac{4\pi l_B}{e_0} \quad (18)$$

$$\Psi'(x=D) = \sigma \frac{4\pi l_B}{e_0} \quad (19)$$

The numerical solution of Eq. 17, taking into account the boundary conditions (Eqs. 18 and 19), yields the equilibrium potential $\Psi(x)$, the equilibrium number densities $n_i(x)$ (Eq. 11) and the probability densities $p_i(s|x)$ (Eq. 10) for different values of parameter

$$P = 2\sigma\pi l_B l_D/e_0 \quad (20)$$

where

$$l_D = \left(\varepsilon \varepsilon_0 kT/8e_0^2 n_0 \right)^{1/2} \quad (21)$$

is Debye length. The definition of the Debye length is equivalent to that of a 2:2 electrolyte containing divalent point-like ions, in our case $l_D = 1$ nm. For comparison, the calculated number densities $n_i(x)$ and corresponding volume charge densities $\rho_i(x)$ between the charged surfaces are determined also by MC simulations, as described in the following section.

MC Simulations

MC simulations were applied in order to check the theoretical predictions of the above-described model. The standard Metropolis algorithm was used in MC simulations (Metropolis et al. 1953), with the periodic boundary conditions in the directions parallel to the charged surfaces for the model, which is schematically shown in Fig. 3. Our system was canonical and consisted of a mixture of positively and negatively charged spheres (there were between 100 and 178 spheres in a box with volume $Y_0^2 D$, where D is the distance between two squared negatively charged surfaces with the surface area Y_0^2). The hard-core interactions between macro-ions and charged walls were taken into account by means of the distance of the closest approach. For consistency with the theory, the hard-core interactions between the particles were neglected. In each MC step, a spherical macro-ion was chosen at random to be randomly rotated around its center or linearly displaced. The selection of the type of the move (orientational or translational) had the same probability. Random linear displacement and random rotation ensure the proper consideration of translational and orientational entropy of the system, respectively (Frenkel and Smith 2002). The shortest distance between positive and negative charges was set to be of the magnitude of Bjerrum length in water to avoid agglutination of oppositely charged particles to each other and consequently to retain the random movement of the particles. On the other hand, due to repulsive forces, the distance between equal charges was considered to be arbitrary. The run time was approximately 5×10^7 MC steps for the whole system of particles. The number of positively and negatively charged macro-ions (N_+, N_-) was determined in accordance with the theory so that the system was kept electroneutral by relation: $Y_0 = [(N_+ - N_-)e_0/\sigma]^{1/2}$. Computation of the electrostatic potential in periodic system with 2D symmetry was performed by the Leckner-Sperb method (Leckner 1991; Sperb 1998), which is the alternative to the Ewald (1921) summation, whereas we used a similar implementation as performed by Moreira and Netz (2002). From MC simulations we obtained number densities of the positive and negative macro-ions between negatively charged surfaces $[\rho_i(x)/e_0 Z]$ as well as their orientation. The average order parameter $S = [3\cos^2(\vartheta) - 1]/2$ within the slices of
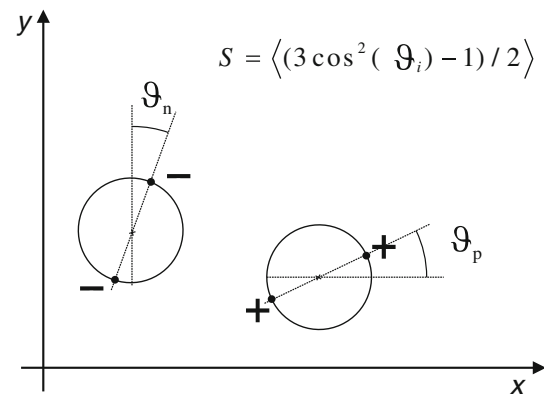

Fig. 4 Schematic definition of the average order parameter S computed from MC simulations. In accordance with the predicted orientation, the angle ϑ_p for positive particles is defined with respect to the x axis, while the angle ϑ_n for negative particles is defined with respect to the y axis. Two charges within the single macro-ion are supposed to be indistinguishable; thus, the two rotational states which are rotated by π are treated equally

thickness $l/2 = 1$ nm along the x-axis direction was calculated to find out how the particles are oriented as a function of variation of the electric field strength in the space between both charged surfaces (Fig. 4). Average order parameter for positively charged particles is defined with respect to the x direction, while for negatively charged particles it is defined with respect to the y direction (Fig. 4). When $S = 0$, it means that particles are not oriented, while $S = 1$ corresponds to particles which are fully oriented with respect to the reference axis.

Results

The density profile of the charge between two negatively charged surfaces is depicted in Figs. 5 and 6 for different values of parameter P (Eq. 20). Good agreement between the theoretical prediction and MC simulations can be seen for low values of $|P|$ (i.e., low $|\sigma|$) as well as for higher values of $|P|$ (i.e., higher $|\sigma|$). In Fig. 6 we can also see the dependence of the average order parameter S on the position between the surfaces. At $x = D/2$, where the electric field strength is $E = 0$, the value of $S = 0$. As the absolute value of E increases in directions to both charged surfaces, also the order parameter S increases in these directions (Fig. 5). In accordance, it can be seen in Fig. 6 that S is the highest when the particle is close to the charged surface. Moreover, we observed differences in average order parameter for different distances between the charged surfaces D (Fig. 7). The values of S for the particles near charged surfaces increase with increasing surface charge density $|\sigma|$. Such behavior of the average orientations of particles together with the fact that the number density of the centers $n_i(x)$ of
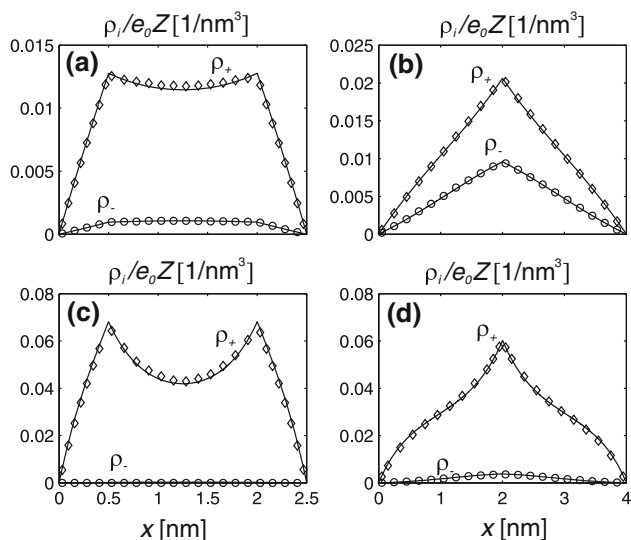
Fig. 5 The volume charge density profile of divalent spherical macro-ions ($l = 2$ nm, $Z = 1$) between two negatively charged membrane surfaces, $\rho_i(x)$, is calculated for two different values of parameter P and two different distances D: **a** $P = -0.1$, $D = 2.5$ nm; **b** $P = -0.1$, $D = 4$ nm; **c** $P = -0.5$, $D = 2.5$ nm; **d** $P = -0.5$, $D = 4$ nm. Theoretical predictions of $\rho_i(x)$ (line) and the corresponding MC results are also given for positive (diamonds) and negative (circles) macro-ions
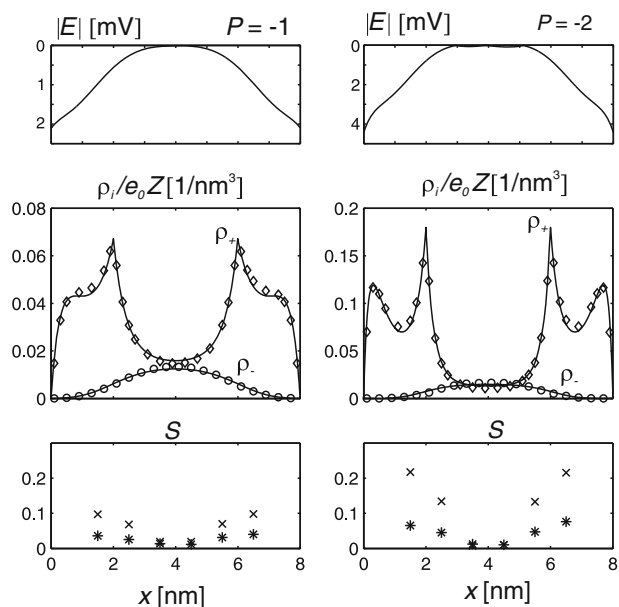

Fig. 7 Dependence of the average order parameter S of positively charged macro-ions on the surface charge density σ for different distances between the charged membrane surfaces (D). In the case of $D = 8$ nm, $Z = 1$ figure shows the value of S in the slice which is closest to the charged surface (see Fig. 6), while in the case of $D = 2.5$ nm the calculated S presents the average value of S in the whole space between the charged surfaces

Fig. 8 Stable equilibrium distances between charged membrane surfaces (D_{eq}) as a function of the diameter of the macro-ion (l) for different charge parameters P and valency $Z = 1$. $\bar{D} = D/l_D$ and $\bar{l} = l/l_D$ are values of the normalized distance between two walls and normalized diameter of the sphere, respectively, in both cases normalized by the Debye length ($l_D = 1$ nm)

Fig. 6 *First row* Electric field, **E**, profile between two negatively charged membrane surfaces computed from mean field theory. *Second row* The volume charge density profile of macro-ions between two negatively charged surfaces. Theoretical predictions (line) are given. Corresponding MC results for positive macro-ions (diamonds) and negative macro-ions (circles). *Third row* The average order parameter S computed in six slices along the x axis for positive macro-ions ($\times$) and negative macro-ions (*). Parameters: $D = 8$ nm, $Z = 1$, $l = 2$ nm, $P = -1$ (left column), $P = -2$ (right column)
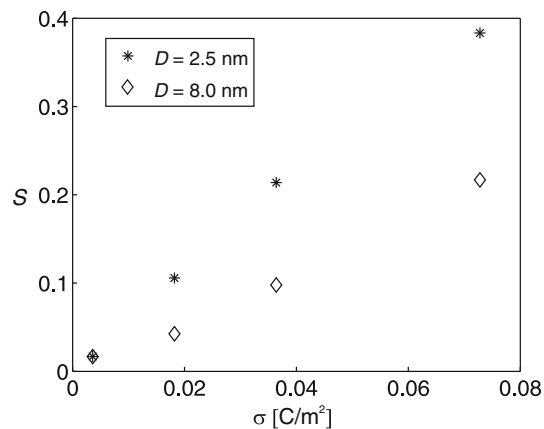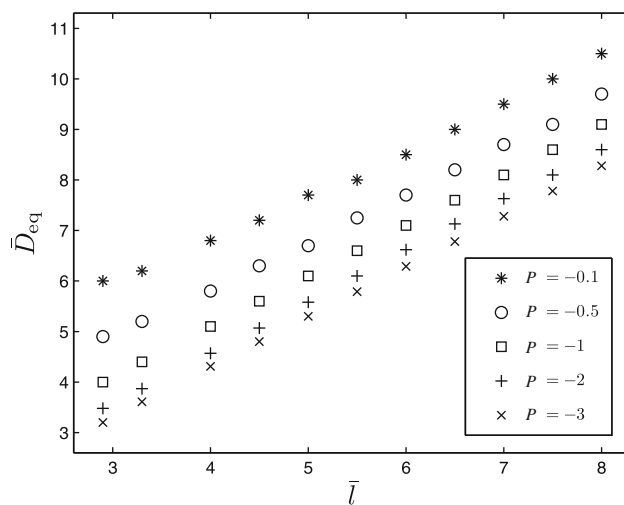
particles is usually the highest at the distance around $l/2$ from the surface contribute to the phenomenon that positively charged particles are trying to bridge negatively charged surfaces at $D \cong l$, as shown in Fig. 8.

Figure 8 shows the equilibrium distances between the charged walls (D_{eq}) where the free energy $F(D)$ exhibits an absolute minimum. The values of D_{eq} are shown as a function of the macro-ion diameter l for different values of the charge parameter P. The results correspond to the

electrostatic bridging, as predicted also in Figure 5a, c. At large diameters the equilibrium distance D_{eq} is approximately equal to the diameters of macro-ions l.

Discussion and Conclusions

As indicated in our study of negatively charged GPVs in solutions with added IgG antibodies (Fig. 2), the antibodies (macro-ions) with internal charge distribution may induce strong adhesion between GPV membranes containing a physiologically relevant number of negative charges. The observed macro-ion-mediated adhesion between equally charged membrane surfaces was also theoretically explained.

Using the functional density theory and MC simulations, we have shown that macro-ions with distinctive internal charge distribution may be strongly oriented in the vicinity of oppositely charged surface, which may lead to bridging forces between equally charged membrane surfaces at their small distances. The predicted equilibrium distances between two negatively charged membrane surfaces (D_{eq}) are only slightly larger than the diameter of the charged macro-ions for sufficiently large macro-ions. Consequently, at equilibrium distance between two negatively charged membrane surfaces there is practically no space for negatively charged macro-ions which are nearly completely depleted from the space between the charged membranes (see Fig. 5a, c), so the bridging attractive interactions mediated by positively charged macro-ions can take place.

The excellent agreement between the predictions of the functional density theory and MC simulations was predicted even at higher values of the coupling constant. This may be explained by the fact that at sufficiently large distances (l) between the two charges within a single divalent macro-ion (see Fig. 3) the charge–charge correlation within the macro-ion (i.e., intraparticle correlation) plays an important role. This is the main reason why the predictions of our functional density theory are in good agreement with the predictions of MC simulations in a large range of model parameters in spite of the fact that the interparticle (inter-ionic) correlations are neglected in the functional density theory. It is therefore expected that the agreement would not be so good for smaller distances between charges l within a single macro-ion (i.e., when the distances between the two charges would be smaller than the diameter of the macro-ion) and especially for point-like particles where the distance between charges l would approach zero.

In the above theoretical analysis we have evaluated the macro-ion-mediated attraction between equally charged surfaces. Our analysis involves a number of approximations;

e.g., we did not take into account the image forces due to different dielectric constants of the aquaues solution of macro-ions and the membrane. Also, we totally neglected the short-range attractive van der Waals forces and the short-range attractive or oscillatory hydration forces between charged surfaces, which might be important if the sugar residues attached to proteins and lipids on the membrane surface do not abolish them (Israelachvili and Wennerström 1996).

In conclusion, we have shown in experiments and within the theoretical predictions (functional density theory and MC simulations) that the adhesion between two equally charged membrane surfaces can be driven by coulombic interactions between the charged surfaces and spherical divalent positive and negative macro-ions. It is indicated that macro-ion-mediated attractive interaction between equally charged surfaces is primarily driven by orientational and positional ordering of divalent positive and negative macro-ions if the distance between the charges within the single macro-ion is large enough.

References

Ambrožič A, Čučnik S, Tomšič N, Urbanija J, Lokar M, Babnik B, Rozman B, Iglič A, Kralj-Iglič V (2006) Interaction of giant phospholipid vesicles containing cardiolipin and cholesterol with ß$_2$-glycoprotein I and anti-ß$_2$-glycoprotein I antibodies. Autoimmun Rev 6:10–15

Angelova MI, Soleau S, Meleard P, Faucon JF, Bothorel P (1992) Preparation of giant vesicles by external AC electric fields. Kinetics and applications. Prog Colloid Polym Sci 89:127–131

Berckmans RJ, Nieuwland R, Tak PP, Bing AN, Romijn FP, Kraan MC (2002) Cell-derived microparticles in synovial fluid from inflamed arthritic joints support coagulation exclusively via a factor VII-dependent mechanism. Arthritis Rheum 46:2857–2866

Bhuiyan LB, Outhwaite CW (2009) Comparison of exclusion volume corrections to the Poisson-Boltzmann equation for inhomogeneous electrolytes. J Coll Int Sci 331:543–547

Bohinc K, Iglič A, May S (2004) Interaction between macro-ions mediated by divalent rod-like ions. Eur Phys Lett 68:494–500

Bohinc K, Slivnik T, Iglič A, Kralj-Iglič V (2008) Membrane electrostatics—statistical mechanical approach to the functional density theory of electric double layer. In: Leitmannova Liu A (ed) Advances in planar lipid bilayers and liposomes, vol 8. Elsevier, New York, pp 107–154

Bohinc K, Zelko J, Kumar S, Iglič A, Kralj-Iglič V (2009) Attraction of like-charged surfaces mediated by spheroidal nanoparticles with spatially distributed electric charge: theory and simulation. In: Leitmannova Liu A (ed) Advances in planar lipid bilayers and liposomes, vol 9. Elsevier, New York, pp 279–301

Carnie S, McLaughlin S (1983) Large divalent cations and electrostatic potentials adjacent to membranes. A theoretical calculation. Biophys J 44:325–332

Celli CM, Gharavi AE, Chaimovich H (1999) Opposite β_2-glycoprotein I requirement for the binding of infectious and autoimmune antiphospholipid antibodies to cardiolipin liposomes is associated with antibody avidity. Biochim Biophys Acta 1416: 225–238

Cerri C, Chimenti D, Conti I, Neri T, Paggiaro P, Celi A (2006) Monocyte/macrophage-derived microparticles up-regulate inflammatory mediator synthesis by human airway epithelial cells. J Immunol 177:1975–1980

Chen S, Liu L, Zhou J, Jiang S (2003) Controlling antibody orientation on charged self-assembled monolayers. Langmuir 19:2859–2864

Combes V, Simon AC, Grau GE, Arnoux D, Camoin L, Sabatier F (1999) In vitro generation of endothelial microparticles and possible prothrombotic activity in patients with lupus anticoagulant. J Clin Invest 104:93–102

Čučnik S, Kveder T, Križaj I, Rozman B, Božič B (2004) High avidity anti-beta 2-glycoprotein I antibodies in patients with antiphospholipid syndrome. Ann Rheum Dis 63:1478–1482

Dachary-Prigent J, Pasquet JM, Freyssinet JM, Nurden AT (1995) Calcium involvement in aminophospholipid exposure and microparticle formation during platelet activation: a study using Ca^{2+}-ATPase inhibitors. Biochemistry 34:11625–11634

Deserno M (2004) Elastic deformation of a fluid membrane upon colloid binding. Phys Rev E 69:031903

Diamant M, Tushuizen ME, Sturk A, Nieuwland R (2004) Cellular microparticles: new players in the field of vascular disease? Eur J Clin Invest 34:392–401

Dignat-George F, Camoin-Jau L, Sabatier F, Arnoux D, Anfosso F, Bardin N (2004) Endothelial microparticles: a potential contribution to the thrombotic complications of the antiphospholipid syndrome. Thromb Haemostasis 91:667–673

Dill KA, Bromberg S (2003) Molecular driving forces. Garland Science, New York

Distler JH, Pisetsky DS, Huber LC, Kalden JR, Gay S, Distler O (2005) Microparticles as regulators of inflammation: novel players of cellular crosstalk in the rheumatic diseases. Arthritis Rheum 52:3337–3348

Ewald PP (1921) Evaluation of optical and electrostatics lattice potentials. Ann Phys (Leipzig) 64:253–287

Fleck CC, Netz RR (2004) Electrostatic colloid-membrane binding. Europhys Lett 67:314–320

Fošnarič M, Iglič A, Kroll DM, May S (2009) Monte Carlo simulations of complex formation between a mixed fluid vesicle and a charged colloid. J Chem Phys 131:105103

Frank M, Manček-Keber M, Kržan M, Sodin-Šemrl S, Jerala R, Iglič A, Rozman B, Kralj-Iglič V (2008) Prevention of microvesiculation by adhesion of buds to the mother cell membrane—a possible anticoagulant effect of healthy donor plasma. Autoimmun Rev 7:240–245

Frank M, Sodin-Šemrl S, Rozman B, Potočnik M, Kralj-Iglič V (2009) Effects of low-molecular-weight heparin on adhesion and vesiculation of phospholipid membranes: a possible mechanism for the treatment of hypercoagulability in antiphospholipid syndrome. Ann N Y Acad Sci 1173:874–886

Frenkel D, Smith B (2002) Understanding molecular simulation from algorithms to applications. Academic Press, London

Góźdź WT (2007) Deformations of lipid vesicles induced by attached spherical particles. Langmuir 23:5665–5669

Greenwalt TJ (2006) The how and why of exocytic vesicles. Transfusion 46:143–152

Hägerstand H, Danieluk M, Bobrowska-Hagerstand M, Pector V, Ruysschaert JM, Kralj-Iglič V, Iglič A (1999) Liposomes composed of a double-chain cationic amphiphile (Vectamidine) induce their own encapsulation into human erythocytes. Biochim Biophys Acta 1421:125–130

Hatlo MM, Lue L (2009) A field theory for ions near charged surfaces valid from weak to strong couplings. Soft Matter 5:125–133

Hill TL (1986) An introduction to statistical thermodynamics. Dover, New York

Ibarra-Armenta JG, Martin-Molina A, Quesada-Perez M (2009) Testing a modified model of the Poisson-Boltzmann theory that includes ion size effects through Monte Carlo simulations. Phys Chem Chem Phys 11:309–316

Israelachvili JN, Wennerström H (1996) Role of hydration and water structure in biological and colloidal interactions. Nature 379:219–225

Janowska-Wieczorek A, Marquez-Curtis LA, Wysoczynski M, Ratajczak MZ (2006) Enhancing effect of platelet-derived microvesicles on the invasive potential of breast cancer cells. Transfusion 46:1199–1209

Kandušer M, Miklavčič D, Pavlin M (2009) Mechanisms involved in gene electrotransfer using high- and low-voltage pulses—an in vitro study. Bioelectrochemistry 74:265–271

Kim YW, Yi J, Pincus PA (2008) Attractions between like-charged surfaces with dumbbell-shaped counterions. Phys Rev Lett 101:208–305

Kirkwood JK, Shumaker JB (1952) The influence of dipole moment fluctuations on the dielectric increment of proteins in solution. Proc Natl Acad Sci USA 38:855–862

Kjellander R (1996) Ion–ion correlations and effective charges in electrolyte and macro-ion systems. Ber Bunsenger Phys Chem 100:894–904

Kralj-Iglič V, Iglič A (1996) A simple statistical mechanical approach to the free energy of the electric double layer including the excluded volume effect. J Phys II France 6:477–491

Leckner J (1991) Summation of coulomb fields in computer-simulated disordered systems. Physica A 176:485–498

Lin AJ, Slack NL, Ahmad A, George CX, Samuel CE, Safinya CR (2003) Three-dimensional imaging of lipid gene-carriers: membrane charge density controls universal transfection behavior in lamellar cationic liposome-DNA complexes. Biophys J 84:3307–3316

Martinez MC, Tesse A, Zobairi F, Andriantsitohaina R (2005) Shed membrane microparticles from circulating and vascular cells in regulating vascular function. Am J Physiol Heart Circ Physiol 288:H1004–H1009

May S, Iglič A, Reščič J, Maset S, Bohinc K (2008) Bridging equally charged macro-ions through long divalent rod-like ions. J Chem Phys B 112:1685–1692

Metropolis N, Rosenbluth AW, Rosenbluth MN, Teller AH, Teller EJ (1953) Equations of state calculations by fast computing machines. Chem Phys 21:1087–1092

Moreira AG, Netz RR (2002) Simulations of counterions at charged plates. Eur Phys J E 8:33–58

Müller I, Klocke A, Alex M, Kotzsch M, Luther T, Morgen-Sternm E (2003) Intravascular tissue factor initiates coagulation via circulating microvesicles and platelets. FASEB J 17:476–478

Netz RR (2001) Electrostatics of counter-ions at and between planar charged walls: from Poisson-Boltzmann to the strong-coupling theory. Eur Phys J E 5:557–574

Oosawa F (1968) Interactions between parallel rodlike macro-ions. Biopolymers 6:1633–1647

Pavlič JI, Mareš T, Bešter J, Janša V, Daniel M, Iglič I (2009) Encapsulation of small spherical liposome into larger flaccid liposome induced by human plasma proteins. Comp Meth Biomech Biomed Eng 12:147–150

Sims PJ, Wiedmer T, Esmon CT, Weiss HJ, Shattil SJ (1989) Assembly of the platelet prothrombinase complex is linked to vesiculation of the platelet plasma membrane. Studies in Scott syndrome: an isolated defect in platelet procoagulant activity. J Biol Chem 264:17049–17057

Sperb R (1998) Alternative to Ewald summation. Mol Simul 20:179–200

Tresset G (2008) Generalized Poisson-Fermi formalism for investigating size correlation effects with multiple ions. Phys Rev E 78:061506

Urbanija J, Tomšič N, Lokar M, Ambrožič A, Čučnik S, Rozman B, Kandušer M, Iglič A, Kralj-Iglič V (2007) Coalescence of phospholipids membranes as a possible origin of anticoagulant effect of serum proteins. Chem Phys Lipids 150:49–57

Urbanija J, Babnik B, Frank M, Tomšič N, Rozman B, Kralj-Iglič V, Iglič A (2008a) Attachment of β_2-glycoprotein I to negatively charged liposomes may prevent the release of daughter vesicles from the parent membrane. Eur Biophys J 37:1085–1095

Urbanija J, Bohinc K, Bellen A, Maset S, Iglič A, Kralj-Iglič V, Sunil Kumar PBS (2008b) Attraction between negatively charged surfaces mediated by spherical counterions with quadrupolar charge distribution. J Chem Phys 129:105101

Whiteside TL (2005) Tumour-derived exosomes or microvesicles: another mechanism of tumour escape from the host immune system? Br J Cancer 92:209–211

Zhou J, Chen S, Jiang S (2003) Orientation of adsorbed antibodies on charged surfaces by computer simulation based on a united-residue model. Langmuir 19:3472–3478